Biophysical Chemistry 151 (2010) 10–21

Contents lists available at ScienceDirect

Biophysical Chemistry

journal homepage: http://www.elsevier.com/locate/biophyschem

Review

What can solid state NMR contribute to our understanding of protein folding?

Kan-Nian Hu, Robert Tycko *

Laboratory of Chemical Physics, National Institute of Diabetes and Digestive and Kidney Diseases, National Institutes of Health, Bethesda, MD 20892-0520, United States

ARTICLE INFO

Article history:
Received 29 April 2010
Received in revised form 18 May 2010
Accepted 18 May 2010
Available online 23 May 2010

Keywords:
Protein folding
Freeze-trapping
Chemical denaturation
Conformational ensembles
Solid state NMR
Villin
HP35

ABSTRACT

Complete understanding of the folding process that connects a structurally disordered state of a protein to an ordered, biochemically functional state requires detailed characterization of intermediate structural states with high resolution and site specificity. While the intrinsically inhomogeneous and dynamic nature of unfolded and partially folded states limits the efficacy of traditional X-ray diffraction and solution NMR in structural studies, solid state NMR methods applied to frozen solutions can circumvent the complications due to molecular motions and conformational exchange encountered in unfolded and partially folded states. Moreover, solid state NMR methods can provide both qualitative and quantitative structural information at the site-specific level, even in the presence of structural inhomogeneity. This article reviews relevant solid state NMR methods and their initial applications to protein folding studies. Using either chemical denaturation to prepare unfolded states at equilibrium or a rapid freezing apparatus to trap non-equilibrium, transient structural states on a sub-millisecond time scale, recent results demonstrate that solid state NMR can contribute essential information about folding processes that is not available from more familiar biophysical methods.

Published by Elsevier B.V.

Contents

1. Introduction . . . 10
2. Solid state NMR of proteins . . . 11
3. Freeze trapping of protein conformations . . . 12
4. Conformational distributions in a helix-forming peptide under chemical denaturation . . . 12
5. Denaturation pathways of the helical model protein HP35 . . . 12
   5.1. Motivations for choosing HP35 . . . 12
   5.2. Qualitative studies of HP35 denaturation . . . 13
   5.3. Site-specific quantitative conformational probes of HP35 denaturation. . . . 13
6. Identification of kinetic folding intermediates . . . 17
7. Related solid state NMR studies . . . 17
8. Future prospects for solid state NMR in protein folding . . . 19
Acknowledgement . . . 19
References . . . 19

1. Introduction

Under physiological conditions, proteins often adopt specific sequence-dependent three-dimensional structures, rather than the random-coil and highly disordered structural states commonly encountered in other kinds of biopolymers and synthetic polymers. The highly ordered structures of proteins are closely related to specific enzymatic functions and molecular signaling cascades that constitute the paradigms of life. It is then intriguing to ask how a protein folds efficiently and reliably to its native structure. Information about the range of unfolded and partially folded structures and the pathways for protein folding is essential for understanding the thermodynamic and kinetic stabilities of proteins and for subsequent engineering manipulations through mutations. Consequently, experimentalists and theorists have addressed the protein folding problem in various ways, with one major goal being the identification and quantification of the structural progression that accompanies folding. Characterization of folding pathways with high structural resolution and time resolution will not only elucidate the stability of important protein folds involved in biological functions, but may also indicate pathological pathways (e.g., leading to

* Corresponding author. National Institutes of Health, Building 5, Room 112, Bethesda, MD 20892-0520, United States. Tel.: +1 301 402 8272; fax: +1 301 496 0825.
E-mail address: robertty@mail.nih.gov (R. Tycko).

0301-4622/$ – see front matter. Published by Elsevier B.V.
doi:10.1016/j.bpc.2010.05.009

disease-associated amyloid aggregation) and suggest potential therapeutic approaches.

Under equilibrium conditions controlled by temperature, pH, or chemical denaturant concentrations, protein folding can be probed by a variety of biophysical measurements including optical absorption and fluorescence spectroscopies, circular dichroism (CD), scattering techniques, and calorimetry. In nonequilibrium experiments, the kinetics of folding can be monitored using spectroscopic and scattering techniques with rapid temporal response [1–7]. While some of these techniques possess sub-microsecond time resolution and can probe the most rapid events in protein folding, they generally provide global, rather than site-specific, structural information.

NMR spectroscopy is a powerful structural tool thanks to the atomic site-specificity of parameters such as chemical shifts and the direct association of parameters such as nuclear magnetic dipole–dipole couplings with molecular structure. The vast majority of protein NMR studies are carried out in the liquid state, where modern multidimensional NMR techniques permit full three-dimensional structure determination with resolution similar to that obtained by X-ray crystallography. Although solution NMR methods have certainly been used effectively to characterize unfolded states of proteins [8–24], dynamical effects complicate the interpretation of NMR spectra of unfolded proteins, preventing direct observation of the underlying conformational components. The alternative approach being explored in our laboratory is to quench the protein and solvent dynamics by freezing (either slowly or rapidly, to create either equilibrium or nonequilibrium states) and to use solid state NMR techniques to characterize the freeze-quenched state [25–28]. As demonstrated below, solid state NMR techniques provide both qualitative and highly quantitative structural information through a variety of structure-dependent parameters. Various components within the static conformational ensemble of an unfolded protein in frozen solution can be resolved spectroscopically or separated by appropriate deconvolution of the solid state NMR data. Even in the presence of structural disorder, well resolved solid state NMR spectra of protein samples can be obtained through site-specific ^{15}N and ^{13}C labeling, combined with the techniques of magic-angle spinning (MAS), proton decoupling, and multidimensional spectroscopy. In the absence of molecular motions, nuclear magnetic dipole–dipole couplings and chemical shift anisotropy (CSA) tensors can be utilized as direct constraints on the interatomic distances and backbone or sidechain torsion angles which are essential for describing the secondary and tertiary structures of proteins.

The following topics are covered in this article: (1) selected principles of solid state NMR methods that are most relevant to protein structural studies; (2) recent progress in the development of solid state NMR methods for qualitative and quantitative characterization of protein conformational distributions in partially folded and unfolded states; (3) recent progress in the development of rapid freezing techniques to trap intermediate states along the pathway from the thermally unfolded state to the folded state of rapidly folding model proteins; (4) prospects for future applications of solid state NMR methods to protein folding and related problems. Much of the presentation below focuses on work from our own research group, mainly because other groups have not yet made similar attempts to apply solid state NMR to protein folding problems. Where possible, relevant work from other groups is also discussed.

2. Solid state NMR of proteins

The excellent atomic-site resolution of NMR results from the long lifetimes of coherences among nuclear spin quantum states, and from the dependence of nuclear spin energies on interactions that include isotropic and anisotropic chemical shifts, magnetic dipole–dipole interactions, electric quadrupolar interactions (present in systems with spin quantum number $>1/2$) and through-bond scalar interactions (i.e., J couplings). In simple liquids and solutions, the rapid molecular tumbling averages out the anisotropic terms in these spin interactions, leaving only the isotropic chemical shifts and J couplings to determine the NMR frequencies. Anisotropic interactions manifest themselves indirectly through nuclear spin relaxation processes (e.g., T_1 and T_2 relaxation, nuclear Overhauser effects). In solids, the anisotropic interactions have direct effects, producing strong dependences of NMR frequencies on molecular orientation. When all possible molecular orientations are present, as in a "powder", the NMR spectra typically contain broad, overlapping lines, with shapes that reflect the details of the orientation dependences (i.e., "powder pattern" lineshapes). Special experimental techniques must therefore be used to obtain high spectral resolution. In organic and biochemical solids, high-resolution ^{13}C and ^{15}N solid state NMR spectra can be recorded using a combination of MAS (i.e., rapid sample rotation about an axis at the angle $\theta_m = \cos^{-1}\left(1/\sqrt{3}\right)\approx 54.7^\circ$ to the external magnetic field, which averages out CSA as well as ^{13}C–^{13}C, ^{15}N–^{13}C, and ^{15}N–^{15}N dipole–dipole couplings) and high-power proton decoupling (i.e., strong irradiation at the ^{1}H NMR frequency to remove ^{1}H–^{13}C and ^{1}H–^{15}N couplings, which are generally too strong to be removed efficiently by MAS alone, especially in the presence of ^{1}H–^{1}H couplings). By concentrating the NMR signal intensity into sharp lines, MAS dramatically improves not only the resolution, but also the sensitivity of NMR measurements on unoriented solids [29–31]. In addition, the sensitivity of ^{13}C and ^{15}N solid state NMR can be enhanced by cross-polarization, which transfers the larger spin polarization of ^{1}H nuclei to ^{13}C or ^{15}N nuclei [32–34].

While the above solid state NMR techniques result in high-resolution spectra by attenuating anisotropic interactions, the ample structural information associated with those interactions is also discarded. It is therefore desirable to "recouple" the anisotropic spin interactions by applying carefully designed, periodic radio-frequency (rf) pulse sequences in synchrony with MAS sample rotation [35–45]. Recoupling techniques allow nuclear magnetic dipole–dipole couplings or CSA to be switched on in certain periods of multidimensional solid state NMR experiments, producing nuclear spin polarization transfers, signal decays, or other effects (e.g., multiple quantum excitation or filtering) that provide information about molecular structure. Particularly for the ^{1}H, ^{13}C, and ^{15}N spin systems that occur in protein samples, pulse sequences have been developed to recouple either homonuclear dipole–dipole interactions [36–39,42,43,45], heteronuclear dipole–dipole interactions [35,41], or CSA interactions [40,44]. Dipole–dipole interactions reflect interatomic distances, which can be either intra-residue distances that depend on sidechain conformations or inter-residue distances that depend on backbone conformations and tertiary structure. CSA interactions reflect the orientations of specific chemical functional groups. Direct constraints on either backbone or sidechain torsion angles can be also obtained from measurements that involve pairs of interactions and hence depend on the relative orientations of two different chemical bonds (pairs of dipole–dipole coupling tensors) [46–48], two different functional groups (pairs of CSA interaction tensors) [49–53], or one bond and one functional group (one dipole–dipole coupling tensor and one CSA interaction tensor) [54–56]. Such measurements are generally called "tensor correlation" techniques.

In addition to quantitative structural constraints that are obtained from precise measurements of dipole–dipole couplings and tensor correlations, qualitative or semi-quantitative constraints on backbone conformations can be obtained from isotropic chemical shifts, especially ^{13}C chemical shifts determined from multidimensional solid state NMR spectra obtained under MAS [57–59]. Semi-quantitative constraints on distances (i.e., inter-residue or intermolecular proximities or contacts) can be obtained from the detection of crosspeak signals in multidimensional spectra that arise from various types of nuclear spin polarization transfer process [60–63]. Distance constraints can also be obtained from measurements of couplings between nuclear spins and electron spins in proteins that contain paramagnetic centers, which can be either intrinsic paramagnetic metal ions or extrinsic spin labels [64,65].

In solid state NMR studies of microcrystalline protein samples, it has been shown that various combinations of the structural constraints mentioned above can be used to develop accurate and complete three-dimensional molecular structures [64,66–69]. Full structural models for noncrystalline samples have also been developed from solid state NMR measurements, with studies of amyloid fibrils being especially noteworthy [59,70–77]. In the case of noncrystalline protein and peptide assemblies, solid state NMR can be the most powerful structural method.

When proteins can be prepared in a highly oriented state, solid state NMR techniques that take full advantage of the orientation dependences of dipole–dipole interactions, CSA interactions, and quadrupole interactions can be used to develop full structural models. Such "oriented-sample" techniques are especially useful in studies of integral membrane proteins and membrane-associated peptides, where a high degree of orientation is achieved through either mechanical or magnetic alignment of phospholipid bilayers [78–81].

3. Freeze trapping of protein conformations

Studies of protein folding by solid state NMR depend on trapping and immobilization of proteins in frozen solutions. Freezing of protein samples to 90–120 K has become routine in X-ray crystallography because it is an efficient way to reduce radiation damage during diffraction measurements with strong synchrotron X-ray sources. Ample discussion of the impact of freezing on protein structures exists in the literature [82–84]. There are two major dangers: (1) formation of crystalline ice particles disrupts protein structures, especially protein–protein interactions and interdomain contacts; (2) cold denaturation of proteins during freezing results in non-native structures. In general, both dangers can be avoided by rapid freezing and by addition of cryoprotectants that suppress solvent crystallization and slow down protein conformational changes through a rapid increase in solvent viscosity with decreasing temperature. Solid state NMR experiments described below were performed with glycerol/water mixtures, with sufficiently high glycerol content that solvent crystallization was suppressed even at low cooling rates (~10 °C per second). With slow cooling, the protein conformation distribution remains at thermal equilibrium until the temperature approaches the solvent glass transition, at approximately −80 °C. Thus, solid state NMR experiments on slowly frozen samples probe the conformational distribution at thermal equilibrium near −80 °C. In contrast, rapid freezing can trap nonequilibrium structural states if the timescale for equilibration (through conformational exchange processes) exceeds the timescale on which the sample temperature falls to values where conformational exchange ceases. In the following sections, we review the initial applications of solid state NMR to proteins in unfolded states produced either by chemical denaturants under equilibrium conditions or by rapid freezing from high temperature under nonequilibrium conditions.

4. Conformational distributions in a helix-forming peptide under chemical denaturation

The first solid state NMR analysis of conformational distributions related to protein folding was attempted by Long and Tycko using the model helix-forming peptide, MB(i+4)EK (N-acetyl-AEAAAKEAAA-KEAAAKA-NH_2), frozen in glass-forming glycerol/water solutions with various urea concentrations and examined at −120 °C [28]. MB(i+4)EK is one of a class of relatively short peptides with high helix contents originally designed by Marqusee and Baldwin [85]. Solid state NMR experiments on MB(i+4)EK were motivated by prior literature on the helix-coil transition in short peptides, which had suggested that 3_{10}-helical conformations might be highly populated under conditions where the overall helix content was low, i.e., that 3_{10}-helices might be intermediates on the folding/unfolding pathways of helical peptides [86]. Solid state NMR studies of MB(i+4)EK used the 2DEXMAS (two-dimensional exchange under MAS) technique, a tensor correlation technique that had been developed previously for quantitative, site-specific backbone torsion angle measurements on polypeptides prepared with ^{13}C labels at two consecutive backbone carbonyl sites [50,52,53]. In 2DEXMAS measurements, information about the backbone ϕ and ψ torsion angles of residue k is contained in the intensities of crosspeak signals that connect MAS sideband lines of carbonyl site k with those of carbonyl site $k-1$ at relatively low MAS frequencies (see below). Experimental crosspeak intensities are analyzed by direct comparison with simulated crosspeak intensities, with the only adjustable parameters being the ϕ and ψ angles and the overall scaling of inter-residue and intra-residue crosspeak intensities.

2DEXMAS data for MB(i+4)EK were acquired at 0.0 M and 5.1 M urea concentrations, where low-temperature circular dichroism spectra indicated overall helix contents of approximately 90% and 63%, respectively. Two peptide samples, with carbonyl ^{13}C labels at A8 and A9 or A13 and A14, were examined to test for possible conformational differences at A9 and A14, i.e., near the middle of the peptide and near the C-terminus. The data were fit with a three-component model for the conformational distributions, comprised of α-helices, 3_{10}-helices, and random coils. For such a model, the conformational distribution is fully described by the fractional populations of α-helices and 3_{10}-helices, $f(\alpha)$ and $f(3_{10})$. Since none of the three components can be adequately described by a single pair of ϕ and ψ values, distributions of ϕ and ψ values for each component were derived from simple molecular dynamics (MD) simulations [28]. Simulated 2DEXMAS data for each component were then calculated from the MD-derived ϕ, ψ distributions. Finally, probabilities that given values of $f(\alpha)$ and $f(3_{10})$ were correct, given the constraints inherent in the experimental data, were evaluated using Bayesian statistics. This analysis led to the conclusions that $f(\alpha)=1.0$ was most probable at 0.0 M urea, and that the most probable distributions at 5.1 M urea had $f(\alpha)+f(3_{10})>0.8$. In other words, MB(i+4)EK was almost entirely α-helical in the absence of denaturant (as expected), but partial disruption of the α-helical conformation by addition of denaturant preferentially produced 3_{10}-helices rather than random coils. The behaviors at A9 and A14 were found to be similar, with possibly larger population of 3_{10}-helical conformations at A9 at 5.1 M urea.

Although these studies were not on a *bona fide* protein and used a simplistic model for conformational distributions, they did demonstrate the potential of solid state NMR to provide quantitative and site-specific structural characterizations of disordered polypeptides. Subsequent studies have further explored and refined this potential, as described below.

5. Denaturation pathways of the helical model protein HP35

5.1. Motivations for choosing HP35

The 35-residue villin headpiece subdomain (HP35) was first identified as a highly stable globular folded structure by McKnight et al. [87] CD measurements identified a thermal unfolding midpoint at 68 °C and a guanidine hydrochloride (GdnHCl) denaturation midpoint at [GdnHCl] = 4.1 M (at 4 °C). The folded structure shown in Fig. 1a was determined first by solution NMR [88] and later by X-ray crystallography [89,90]. HP35 contains three α-helical segments (underlined in the amino acid sequence LSDEDFKAVFGMTRSAFANL PLWKQQNLKKEKGLF, conventionally numbered 42–76). Local helix contents predicted by AGADIR [91] are less than 5% at 4 °C, suggesting that strong secondary structure propensities alone do not explain the stability of the folded state. Sidechains of L42, F47, V50, F51, F58, L61, and L75 form a hydrophobic core that presumably accounts for much of the stability [92], along with the weak helix propensities and possibly other factors.

The kinetics of HP35 folding have been addressed by time-resolved fluorescence measurements with rapid temperature-jump methods [1,2,93,94], as well as by dynamical NMR [95] and time-resolved

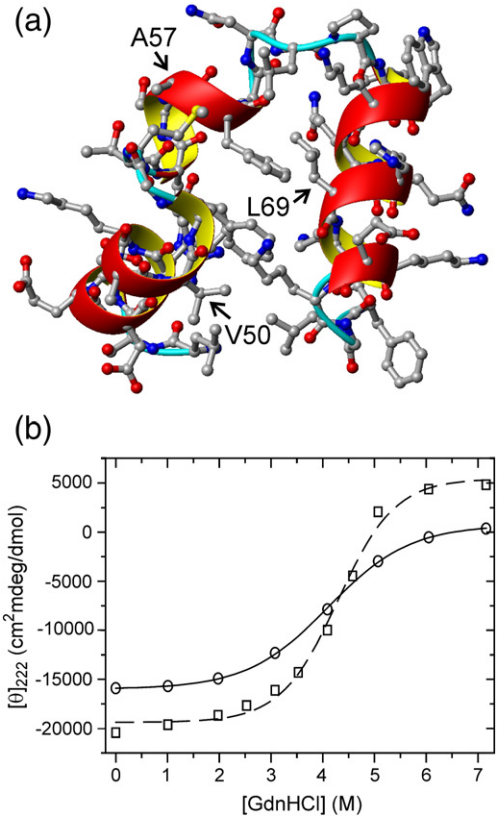

Fig. 1. (a) Structure of villin HP35 in the folded state (PDB 1YRF). A ribbon representation is superimposed on the atomic structure to show the three helical segments. (b) Denaturation of HP35 in glycerol/water by addition of GdnHCl, monitored by circular dichroism at 222 nm. Circles and squares are data at 22 °C and −55 °C, respectively. Solid and dashed lines are fits with a simple two-state model, which yield denaturation midpoints equal to 4.1 ± 0.1 M at 22 °C and 4.3 ± 0.2 M at −55 °C, and unfolding free energies at [GdnHCl] = 0.0 M equal to 3.07 ± 0.08 kcal/mol at 22 °C and 3.38 ± 0.39 kcal/mol at −55 °C.

infrared [96] measurements. Fluorescence measurements on the N60H mutant of HP35 indicate a 5 μs time scale for folding between 32 °C and 80 °C [2]. The corresponding time scale near 60 °C estimated from exchange broadening effects in solution NMR spectra of the 36-residue version of the wild-type subdomain (HP36) is 5–10 μs [95]. Infrared measurements with site-specific isotopic labeling show a very rapid phase of structural relaxation (~0.1 μs) in addition to a 5 μs phase at 45 °C [96]. The apparently rapid folding kinetics and small size of HP35 (or HP36) combine to make it a popular target for theoretical and computational studies of protein folding [97–106], including efforts to simulate the entire folding process with atomic detail. For our own work, the small size permits site-specific isotopic labeling by solid phase peptide synthesis.

5.2. Qualitative studies of HP35 denaturation

In initial solid state NMR studies of HP35, 2D ^{13}C–^{13}C spectra of a sample that was ^{13}C-labeled at all carbon sites in selected residues were recorded in frozen glycerol/water with varying concentrations of GdnHCl [27]. Samples for solid state NMR were frozen relatively slowly (roughly 10 °C per second), by immersing the MAS rotor that contained the HP35 solution in liquid nitrogen. CD spectroscopy was also used to determine the denaturation midpoint in glycerol/water at temperatures between 20 °C and −40 °C (later extended to −55 °C [26]). Suprisingly, the denaturation midpoint was found to be [GdnHCl] = 4.2 ± 0.2 M over the entire temperature range (see Fig. 1b). Thermodynamic parameters derived by fitting the CD data with a simple two-state model did not vary significantly with temperature and were essentially the same as the corresponding parameters at 4 °C in the absence of glycerol. Moreover, all solid state NMR data [26,27] indicate a denaturation midpoint near [GdnHCl] = 4.5 M. With slow freezing, one expects the protein conformational distribution to remain at thermal equilibrium until the sample temperature approaches the glass transition temperature of the glycerol/water solvent ($T_g \approx -80$ °C). The fact that denaturation of HP35 in glycerol/water is nearly independent of temperature over a range of nearly 100 °C remains to be explained, but supports the idea that solid state NMR experiments on frozen protein solutions at low temperatures are relevant to protein folding in fluid solutions.

^{13}C signals of individual sites in selectively labeled HP35 were clearly resolved in the 2D ^{13}C–^{13}C spectra (see Fig. 2). At [GdnHCl] = 0.0 M, ^{13}C chemical shifts of V50, A57, and L69 were consistent with the expected helical secondary structure of folded HP35. Moreover, the two methyl sites of Val50 showed sharp, resolved signals indicative of ordered sidechain conformations. Thus, "cold denaturation" of HP35 did not take place even with slow cooling.

Addition of GdnHCl had a profound effect on the 2D spectra. Between [GdnHCl] = 4.0 M and [GdnHCl] = 5.0 M, all crosspeak signals in these spectra shifted and generally became broader. Because signals from individual sites were resolved in the 2D spectra, the solid state NMR data clearly showed that denaturation was not fully synchronized in the three helical segments of HP35, inconsistent with a simple two-state denaturation process, even though data from optical techniques such as CD and fluorescence spectroscopy could be fit with simple two-state models. For example, as shown in Fig. 2c, solid state NMR signals from V50 reached their unfolded limit at [GdnHCl] = 5.0 M, while signals from A57 were still intermediate between their folded and unfolded limits.

Effects of secondary and tertiary interactions on the stability of HP35 were separated by recording 2D solid state NMR spectra of peptides that encompass the individual helical segments (residues 42–52, 53–61, and 62–76). Spectra of equimolar mixtures of the three peptides with variable GdnHCl concentrations, also labeled at V50, A57, and L69, were similar to those of the intact protein but with reduced helix content at L69 at [GdnHCl] = 0.0 M and with more pronounced site-specific variations in the apparent denaturation midpoint. All 2D spectra of intact HP35 could be fit quite well with a "two-step" model [27], in which the spectrum at each GdnHCl concentration was represented by a superposition of the fully-folded protein spectrum and the peptide spectrum *at the same GdnHCl concentration* (rather than a superposition of the fully-folded protein spectrum and the fully-denatured protein spectrum). This model suggests that HP35 denaturation can be considered to occur in two steps: (i) disruption of tertiary interactions in a fraction of HP35 molecules by the denaturant, creating a mixture of folded and unfolded molecules; (ii) independent equilibration of secondary structure within each helical segment of the unfolded molecules, resulting in site-dependent and denaturant-dependent helix contents that produce non-two-state behavior.

5.3. Site-specific quantitative conformational probes of HP35 denaturation

The initial experiments on HP35 described above established the feasibility of solid state NMR measurements on partially folded and unfolded proteins in frozen solutions. These experiments also demonstrated that new information could be obtained through the site-specific sensitivity of solid state NMR to local structural changes, in the form of new insights into the mechanism of chemical denaturation. A second set of experiments on HP35 were then designed to test whether solid state NMR methods could provide quantitative information about site-specific conformational distributions in partially folded and unfolded states [26]. These experiments employed three solid state NMR techniques that had been developed earlier for structural studies of structurally ordered proteins and peptides, namely 2D exchange spectroscopy with magic-angle spinning (2DEXMAS) [50,52,56], constant-time double-quantum-filtered dipolar recoupling (CTDQFD) [107], and double-quantum chemical shift anisotropy spectroscopy

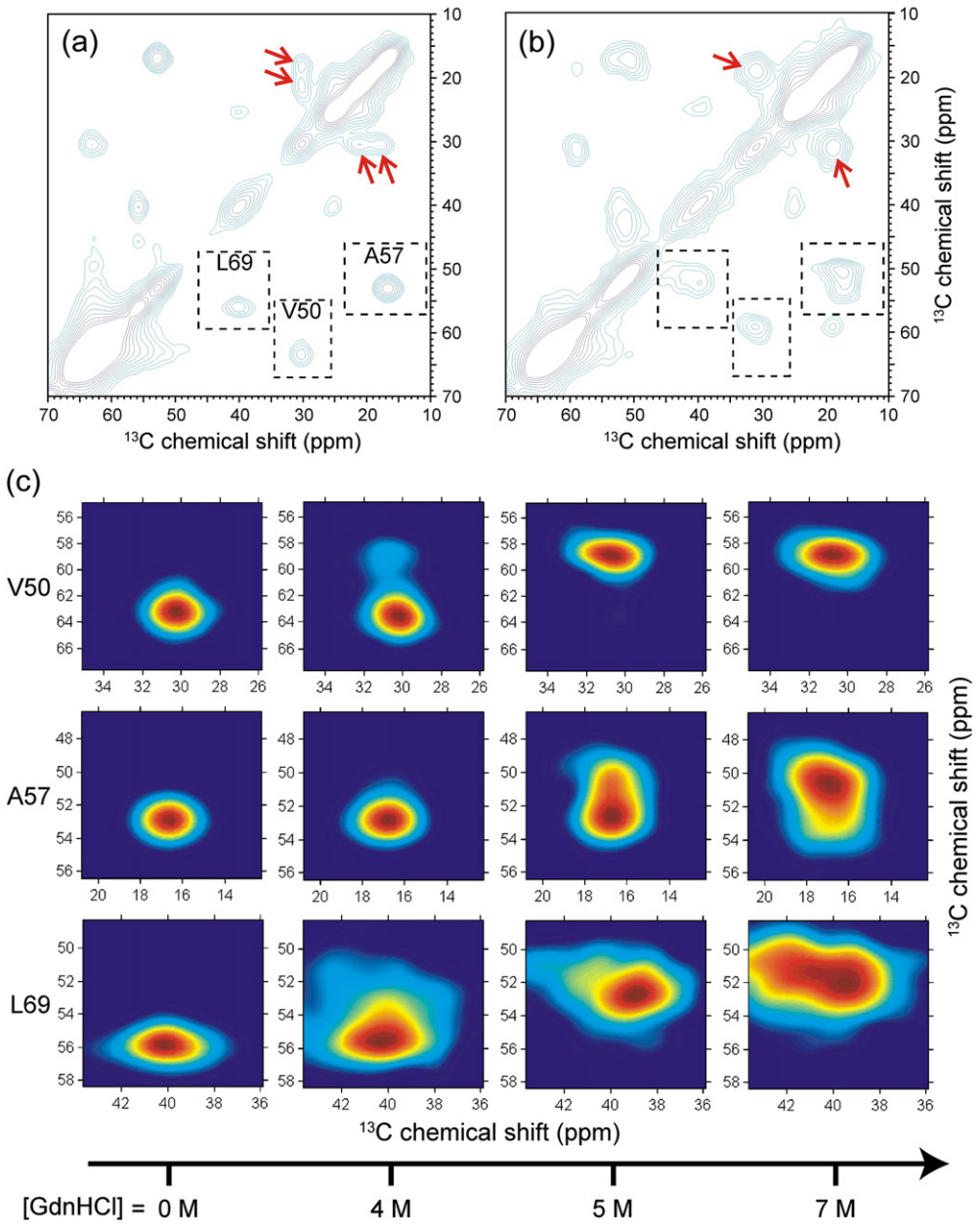

Fig. 2. Chemical denaturation of HP35 monitored at the site-specific level by 2D solid state NMR. (a) Aliphatic region of the 2D ^{13}C–^{13}C spectrum in frozen glycerol/water with [GdnHCl] = 0.0 M. C_α/C_β crosspeak signals of the uniformly ^{13}C-labeled residues V50, A57, and L69 (one residue in each helical segment of HP35) are located in the dashed boxes. Red arrows indicate C_β/C_γ crosspeaks of V50, which are split due to inequivalence of the two V50 methyl carbons in the folded state. (b) Aliphatic region of the 2D ^{13}C–^{13}C spectrum in frozen glycerol/water with [GdnHCl] = 7.0 M. In this fully denatured state, C_α/C_β crosspeaks are shifted and broadened, reflecting non-helical and disordered secondary structure. A single, broader C_β/C_γ crosspeak is observed for V50, reflecting the absence of native tertiary structure. (c) Dependence of C_α/C_β crosspeak signals on denaturant concentration. Loss of helical secondary structure occurs between 4.0 M and 5.0 M, but not simultaneously at all three labeled residues.

(DQCSA) [49]. All three techniques are applicable to proteins that are ^{13}C-labeled at sequential pairs of backbone carbonyl sites (i.e., residues $k-1$ and k), and all three techniques yield quantitative constraints on the backbone torsion angles ϕ and ψ between the two labeled site (i.e., ϕ and ψ of residue k), as shown in Fig. 3a. Rf pulse sequences and examples of the resulting data are shown in Fig. 3b–f. In the case of 2DEXMAS measurements, conformational information is contained in the amplitudes of crosspeaks that connect MAS sidebands of the two labeled carbonyls. In the case of CTDQFD measurements, conformational information is contained in the build-up and decay of double-quantum-filtered ^{13}C NMR signals (i.e., signals that arise from coherent superpositions of nuclear spin states that differ by spin flips at both labeled sites) in an evolution period during which dipole–dipole interactions between labeled pairs are recoupled under MAS. In the case of DQCSA measurements, conformational information is contained in the decay of double-quantum filtered signals in an evolution period during which CSA interactions of both carbonyl sites are recoupled. 2DEXMAS and DQCSA data are sensitive to the relative orientations of the two labeled carbonyl groups, and hence depend strongly on both ϕ and ψ. CTDQFD data depend primarily on the ^{13}C–^{13}C distance, and hence depend more strongly on ϕ than on ψ. For all three techniques, earlier applications to model peptides had verified that the data could be analyzed accurately by comparison with numerical simulations of the nuclear spin evolution under the relevant rf pulse sequences [49,50,53,107].

2DEXMAS, CTDQFD, and DQCSA data were obtained for HP35 samples that were ^{13}C-labeled at A49 and V50 (to probe ϕ and ψ of V50 in the first helical segment of HP35), S56 and A57 (to probe ϕ and ψ of A57 in the second helical segment), or L69 and K70 (to probe ϕ and ψ of

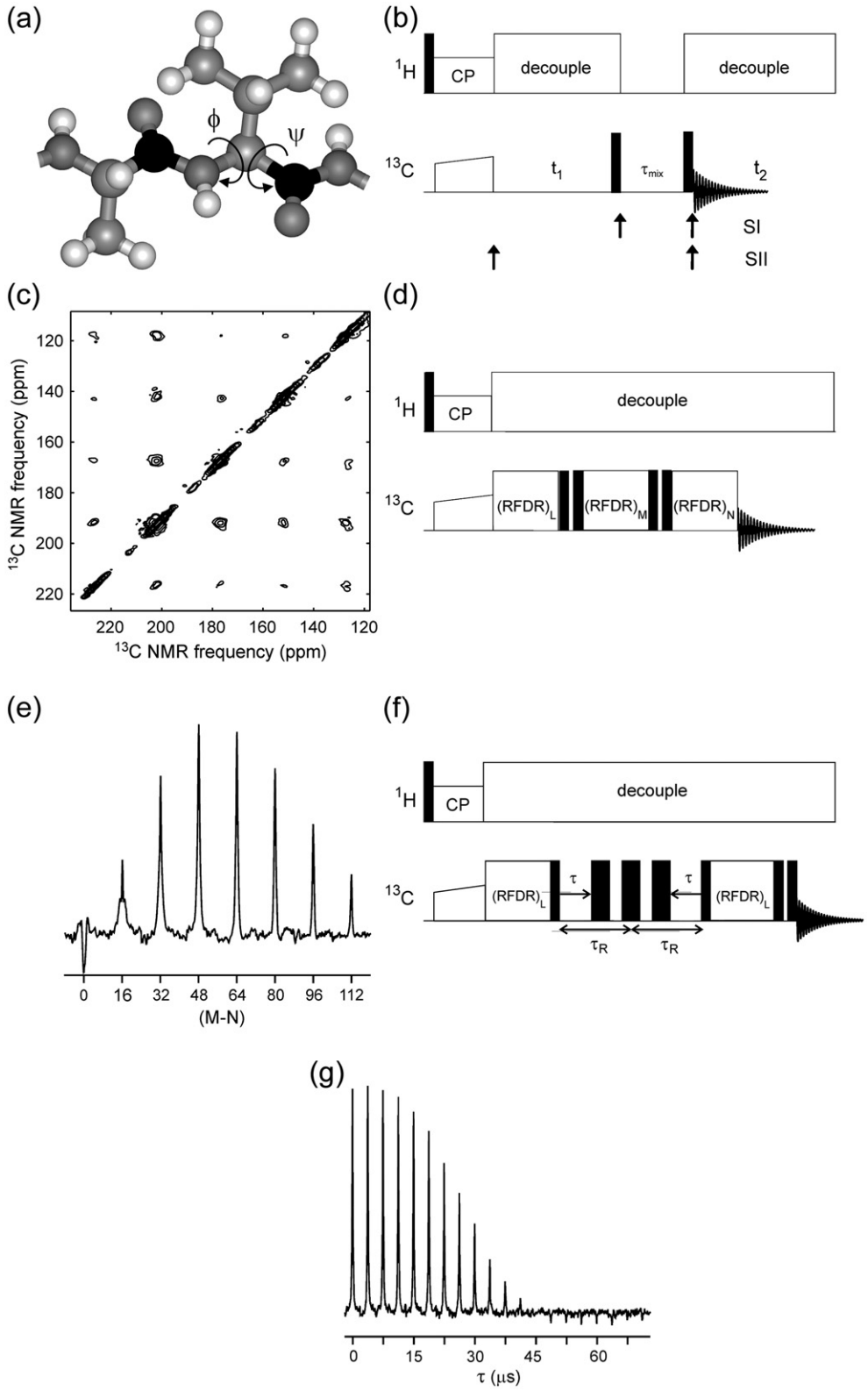

Fig. 3. Solid state NMR techniques for quantitative measurements of backbone ϕ and ψ torsion angles. (a) Section of a polypeptide backbone with ^{13}C labeling at carbonyl sites (black spheres) of consecutive Ala and Val residues. Solid state NMR data place constraints on ϕ and ψ angles between the two labels. (b) Rf pulse sequence for 2DEXMAS measurements, showing pulses on ^{1}H and ^{13}C channels. Black bars represent $\pi/2$ pulses. CP = cross-polarization. (c) 2DEXMAS spectrum of HP35 in frozen glycerol/water with [GdnHCl] = 0.0 M, recorded at 100.8 MHz ^{13}C NMR frequency with magic-angle spinning at 2.50 kHz and $\tau_{mix} = 500$ ms. Intensities of crosspeak signals, which connect MAS sidebands of the two labeled sites (A49 and V50), depend on the relative orientations of the carbonyl groups, hence on ϕ and ψ. This spectrum is obtained by combining data sets with rf pulse timing such that either τ_{mix} or $\tau_{mix} + t_1$ is a multiple of the MAS rotation period τ_R (signals SI and SII). (d) Rf pulse sequence for CTDQFD measurements, with $(RFDR)_N$ representing a ^{13}C–^{13}C dipolar recoupling period of duration $N\tau_R$. Rf phase cycling (not shown) selects signals that arise from double-quantum coherences involving the ^{13}C-labeled carbonyl pairs. (e) CTDQFD data for A49,V50-labeled HP35. Build-up and decay of carbonyl signal intensities with increasing M–N depends on ϕ and ψ. (f) Rf pulse sequence of DQCSA measurements. Thicker black bars represent π pulses that recouple chemical shift anisotropies. Rf phase cycling (not shown) selects signals that arise from double-quantum coherences involving the ^{13}C-labeled carbonyl pairs. (g) DQCSA data for A49,V50-labeled HP35. Decay of carbonyl signals with increasing τ depends on ϕ and ψ.

K70 in the third helical segment). Data were obtained in frozen glycerol/water solutions with [GdnHCl] = 0.0 M, 4.5 M, and 7.0 M, representing the fully folded condition, the approximate denaturation midpoint, and the strongly denatured condition. At [GdnHCl] = 0.0 M, data for all three samples could be fit with single ϕ, ψ values that agree well with values for the same sites in HP35 crystal structures. At [GdnHCl] = 4.5 M and 7.0 M, the data could not be fit adequately with single ϕ, ψ values, consistent with the presence of conformational distributions in the partially and fully denatured states.

Conformational distributions that fit the solid state NMR data were obtained by invoking two models [26]. In the first model, the distributions were approximated by small numbers of populated regions in the ϕ, ψ plane, with each region having a two-dimensional Gaussian shape. Variable parameters were the number of regions (one, two, or three), the centers and widths of each Gaussian functions, and the relative volumes of the Gaussian functions. Data could be simulated for any choice of these parameters, and the agreement between experimental and simulated data was described by χ^2 values, normalized to experimental uncertainties in order to be statistically meaningful. Parameters that produced acceptably low χ^2 values were found by a simulated annealing algorithm, and ranges of acceptable parameters were evaluated by Markov-chain Monte Carlo (MCMC) simulations. Results of the data analysis with this "multiple Gaussian" model are shown in Fig. 4. Surprisingly, for all three HP35 samples, the data at [GdnHCl] = 4.5 M and 7.0 M could be fit with only two relatively narrow populated regions, indicating two predominant backbone conformations at the labeled sites. At [GdnHCl] = 4.5 M, one region was centered at α-helical ϕ, ψ values, as expected. The other region was near $\phi \approx -120°$ and $\psi \approx 80°$ (with significant site-specific variations), corresponding to extended backbone conformations that approach β-strands. At [GdnHCl] = 7.0 M, the two populated regions were found to correspond to extended conformations and polyproline II (PPII) conformations ($\phi \approx$ -80° and $\psi \approx 160°$). At [GdnHCl] = 4.5 M, PPII conformations were not significantly populated, as the χ^2 value was not reduced significantly by using three Gaussian functions instead of two.

In the second model, conformational distributions were approximated by a large number of populated points in the ϕ, ψ plane. Variable parameters, again optimized by simulated annealing, were the position of each point and the number of points. For distributions with low χ^2, most points in this "multiple point" model were located in the same ϕ, ψ regions that were populated in the "multiple Gaussian" model. The fact that two quite different models yielded similar conformational distributions indicates that the results are not merely model-dependent.

These results for HP35 suggest an "unfolding pathway" under chemical denaturation [26], shown in Fig. 4. As denaturant is added to the protein solution, residues in helical segments first convert preferentially to extended conformations. As the denaturant concentration becomes high, the same residues begin to populate PPII conformations and stop populating helical conformations. Considerable literature, both experimental [108–113] and theoretical [114,115], has suggested that conformational distributions in denatured states of proteins contain high populations of extended and PPII conformations. The results from solid state NMR generally support this picture, but were obtained without relying on previous suggestions or assumptions. The "pathway" suggested by solid state NMR experiments has not been identified in previous studies. Moreover, it is important to recognize that conformational distributions derived by fitting data such as 2DEXMAS, CTDQFD, and DQCSA data do not depend in any way on information from structural databases (e.g., the random coil libraries that have been used in previous studies [11,19,22]), from molecular modeling [20], or from "intuition" regarding the structural propensities of polypeptides. Conclusions from quantitative solid state NMR measurements follow

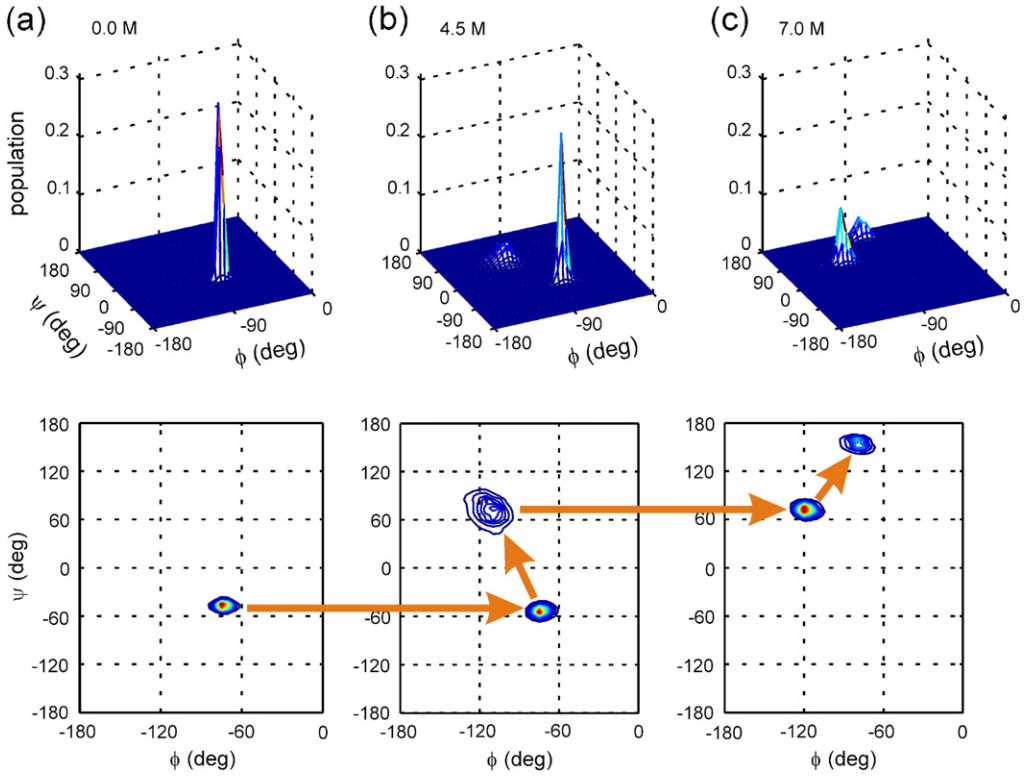

Fig. 4. Analyses of combined 2DEXMAS, CTDQFD, and DQCSA data for A49,V50-labeled HP35 in frozen glycerol/water. For each value of [GdnHCl], the three data sets are fit simultaneously with a "multiple Gaussian" model for the ϕ, ψ distribution at V50. (a) Data at [GdnHCl] = 0.0 M are fit adequately by a single Gaussian function, centered at α-helical ϕ, ψ values. (b) Data at [GdnHCl] = 4.5 M require two Gaussian functions, centered at α-helical and partially extended ϕ, ψ values. (c) Data at [GdnHCl] 7.0 M require two Gaussian functions, centered at partially extended and polyproline II ϕ, ψ values. For each value of [GdnHCl], distributions shown as surface plots (top) and contour plots (bottom) are averages of all distributions that fit the data adequately, as determined by Markov chain Monte Carlo simulations. Orange arrows indicate the denaturation "pathway" revealed by the solid state NMR data, in which α-helical conformations convert first to partially extended conformations, and then to polyproline II conformations.

simply from fitting experimental NMR signal intensities to numerical simulations of NMR measurements, which depend only on chemical bond lengths and bond angles, NMR chemical shifts that are determined from experiments, and rf pulse sequence conditions.

Identification of the "pathway" in Fig. 4 depends on the ability to deconvolve the signals of folded molecules from those of unfolded molecules, and to deconvolve various components within the unfolded ensemble. Rapid conformational exchange makes such a deconvolution difficult in solution NMR. In principle, vibrational spectroscopies may be able to provide similar information, especially with isotopic labeling of specific backbone sites, but quantitative analysis of vibrational spectra in terms of backbone torsion angles is not straightforward. In future solid state NMR studies, it will be interesting to examine the denaturation "pathways" for other model proteins, including those with β-sheet secondary structures.

6. Identification of kinetic folding intermediates

Experiments on HP35 described above provide detailed information about structural changes that occur at equilibrium, as solvent conditions change from those that favor the folded state to those that favor a more disordered state. A more challenging goal, and one that relates directly to many current computational and experimental studies of protein folding, is to use solid state NMR to track the time dependence of structural changes following a rapid change in conditions (e.g., pH, pressure, or temperature). We have recently reported the first example of such a study, in which a transient intermediate state of HP35 was trapped by rapid freezing from a thermally unfolded state and subsequently characterized by solid state NMR [25].

The rapid folding kinetics of HP35 require freezing on the submillisecond time scale. For this purpose, a relatively simple apparatus was developed for heating an appropriate volume of protein solution to temperatures up to 90 °C, pumping the heated solution through a 20 μm-diameter aperture to create a fine jet of solution traveling at 10^4 cm/s, and freezing the solution in stirred isopentane at −140 °C [25]. Direct imaging of the resulting slurry of frozen solution revealed that it consisted of particles with diameters of approximately 10 μm. Numerical calculations of the cooling of water/glycerol particles indicated that the time to pass from 90 °C to 0 °C was 10–20 μs for most of the volume, depending on distance from the particle surface. Additional parts were constructed so that the frozen protein solution could be separated from the isopentane and packed in a MAS rotor, while maintaining the sample temperature below −120 °C at all times. Experimental measurements confirmed that protein folding was effectively quenched during sample preparation and subsequent solid state NMR measurements, and that cooling of the heated protein solution occurred almost entirely during the initial immersion in cold isopentane (rather than during the 100–200 μs travel time from the aperture to the isopentane surface). Related approaches to rapid freezing have been developed by other groups for related purposes in magnetic resonance and other spectroscopies [116–118].

Fig. 5a and b compare 1D ^{13}C NMR spectra of selectively-labeled HP35, frozen rapidly from the folded state at 24 °C or from the unfolded state at 90 °C. Rapid freezing from the folded state results in a spectrum with relatively sharp lines at chemical shifts that are consistent with the expected helical secondary structure. The splitting of V50 methyl signals discussed above is clearly resolved. In contrast, rapid freezing from the unfolded state results in a spectrum with broader lines and without a resolved splitting of V50 methyl signals. Clearly, despite the reported 5 μs folding time for HP35 in aqueous solution and the estimated 10–20 μs freezing time in our experiments, a state that is at least partially unfolded was trapped in these experiments.

Fig. 5c and d compare 2D ^{13}C NMR spectra of selectively-labeled HP35 in the folded state and in the freeze-trapped state. A single set of relatively sharp crosspeaks is observed in the folded state. In the freeze-trapped state, crosspeak signals can be divided into two components. The first component is broad, and located at chemical shifts that differ significantly from those of the folded state. This component is assigned to strongly unfolded HP35 molecules. The second component is sharper, and located at chemical shifts that are similar to those of the folded state, suggesting that it arises from folded molecules. However, the second signal component is not identical to folded state signals. In particular, no splitting of V50 methyl signals is observed. Thus, no fully folded HP35 molecules are detectable in solid state NMR spectra of the freeze-trapped state.

Our current interpretation of these results is that folding of HP35 (and perhaps other rapidly-folding proteins and protein domains) from a thermally unfolded state occurs in two phases, as depicted in Fig. 6. The initial, rapid phase involves conversion of strongly disordered molecules to a partially folded intermediate state with native-like secondary structure but incomplete tertiary structure. The intermediate state includes a distribution of conformations. In aqueous solution and in the 32–80 °C temperature range, this process would require approximately 5 μs, corresponding to the folding process seen in temperature-jump fluorescence measurements [2]. In the more viscous glycerol/water solutions used in our experiments (with strongly temperature-dependent viscosity), this process is slowed to the point where a mixture of strongly disordered and partially folded molecules can be trapped in the 10–20 μs freezing time. The second phase entails the conversion of partially folded molecules to fully folded molecules with ordered tertiary structure, a process that requires conformational rearrangements that are impeded by free energy barriers [97]. The time scale of the second phase can be considerably longer than that of the first phase. Under the conditions of our experiments, the time scale of the second phase apparently exceeds 10–20 μs, as fully folded molecules are not observed. The second phase may not produce measureable changes in fluorescence quantum yields.

Additional experimental evidence for the intermediate state comes from additional 2D spectra of freeze-trapped HP35 and from measurements of tertiary contacts by ^{13}C–^{13}C polarization transfer [25]. On the computational side, Freddolino et al. have recently reported all-atom MD simulations of HP35 folding in water in which intermediate states with native-like secondary structure but non-native tertiary structure are observed in several long trajectories [106]. These intermediate states have structural properties that are generally consistent with our solid state NMR data for freeze-trapped HP35. Conversion of the intermediate states to the final folded state occurs at 5.6–8.2 μs in the simulations, significantly later than the average folding time suggested by temperature-jump fluorescence measurements. The still longer lifetime indicated by our experiments may be a consequence of the higher viscosity in the experiments and (to a lesser extent) the fact that the simulations were performed on the N60H mutant. Imperfections in the MD potentials may also contribute to discrepancies between simulated and experimental time scales. Partially folded intermediates have also been observed in other computational studies of HP35 folding [97].

7. Related solid state NMR studies

Several studies by other groups are relevant to the protein folding studies discussed above. Etzkorn et al. [119] have reported solid state NMR studies of the Crh protein in which a native-like, but noncrystalline, precipitate was first prepared at −4 °C. Upon heating to 9 °C, the Crh sample gradually converted to an insoluble aggregated state with lower helical and higher β-sheet secondary structure. The structural conversion process was monitored by 2D solid state ^{13}C NMR, which revealed large chemical shift changes for specific sites where the secondary structure changes occurred. This work indicates how an unfolding process could be studied with site-specific detail.

Ishii and coworkers have used solid state NMR measurements to examine the conformation and β-sheet structure of metastable oligomeric aggregates of the β-amyloid peptide, which typically precede the appearance of β-amyloid fibrils when fibrils form from the monomeric

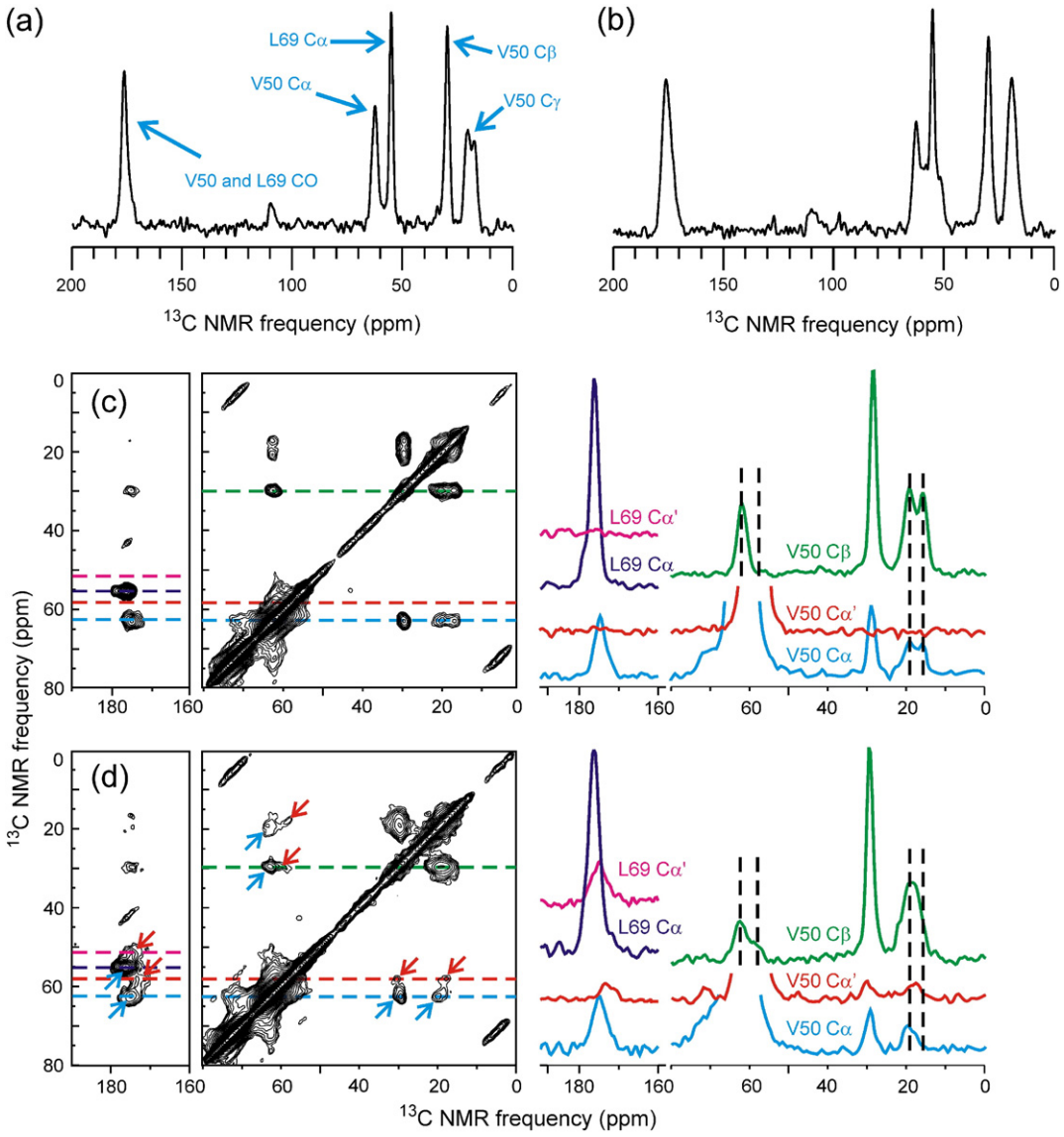

Fig. 5. Evidence for a freeze-trapped intermediate state in the folding process of HP35. (a) 1D ^{13}C NMR spectrum of HP35 in glycerol/water after rapid freezing from 24 °C. The protein is ^{13}C labeled at CO and C_α sites of L69 and at all carbon sites of V50. Double-quantum filtering is used to suppress natural-abundance ^{13}C NMR signals from glycerol. Slow freezing from 24 °C yields nearly the same spectrum. (b) 1D ^{13}C NMR spectrum after rapid freezing from 90 °C. Broader lines and other changes demonstrate that a non-equilibrium structural state is trapped by rapid freezing. (c) 2D ^{13}C–^{13}C NMR spectrum after slow freezing from 24 °C, with color-coded 1D slices to the right. (d) 2D ^{13}C–^{13}C NMR spectrum after rapid freezing from 90 °C. Red arrows indicate signals from strongly unfolded molecules. Cyan arrows indicate signals from partially folded molecules. The absence a splitting of V50 C_γ signals in the V50 C_α and C_γ slices (cyan and green) shows that partially folded molecules are not fully folded.

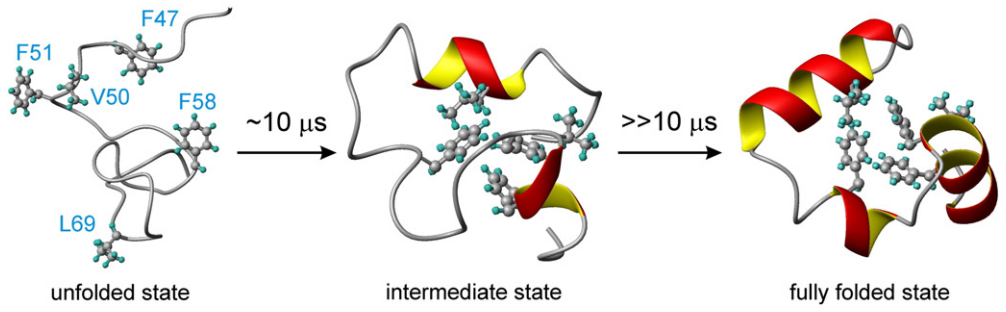

Fig. 6. Picture of HP35 folding that emerges from solid state NMR data. Starting from a strongly unfolded state at high temperatures, rapid cooling to below the thermal unfolding temperature (74 °C mid-point in glycerol/water) leads to conversion to a partially folded intermediate state on the 10–20 μs time scale. The intermediate state has a high population of native secondary structure, but lacks fully ordered tertiary structure. Conversion to the fully folded state occurs on a longer time scale. Rapid freezing to below the solvent glass transition temperature prevents this second stage of folding.

peptide [120]. In the specific oligomer morphology examined by Ishii and coworkers in a lyophilized state, the peptide conformation and β-sheet structure (indicated by ^{13}C chemical shifts and intermolecular dipole–dipole couplings) are remarkable similar to those in mature fibrils. In future work, freeze-trapping techniques could be used to arrest the evolution of β-amyloid aggregates at various stages, allowing full characterization of intermediate structural states [121]. Such studies would potentially be of great interest, as recent literature suggests that the primary neurotoxic form of the β-amyloid peptide could be anywhere from a dimer to a mature fibril.

Solid state NMR techniques have also been used extensively to characterize structural changes in the light-driven proton pumping cycle of bacteriorhodopsin [122,123] and the photoactivation of mammalian rhodopsin [124,125]. To date, these studies have used continuous optical irradiation and low temperatures to prepare photocycle intermediates at steady state. In principle, rapid freezing techniques as described above could be used to trap transient intermediates after initiation of structural changes by pulsed optical excitation.

The general problem of extracting conformational distributions from quantitative solid state NMR measurements has been addressed by Utz [126], who developed a mathematic formalism for relating specific patterns of data ("eigenspectra") to basis functions for the distribution. In the absence of noise, Utz's formalism can be used to derive a unique conformational distribution directly from the data, without invoking models such as the "multiple Gaussian" and "multiple point" models discussed above. When noise or other random errors are not negligible, such a direct analysis does not produce useful results. Fitting the experimental data with physically reasonable models for the conformational distribution becomes a better approach. Nonetheless, Utz's formalism provides a mathematically justified method for assessing the potential information content of each structural technique.

8. Future prospects for solid state NMR in protein folding

Results discussed above amply demonstrate the potential of solid state NMR methods to provide new information about protein folding, including the detailed nature of conformational distributions in partially folded and unfolded states at equilibrium and the time-dependence of structural distributions after sudden changes in solvent conditions. This information derives from several unique features of NMR measurements, including their sensitivity to local structural details and their ability to monitor structural properties at multiple sites simultaneously (due to high spectral resolution, aided by multidimensional spectroscopy). Solid state NMR in particular offers the advantage of structural techniques, including various dipolar recoupling, CSA recoupling, and tensor correlation techniques, that are highly quantitative and hence can be analyzed mathematically even in the presence of structural distributions. Simple measurements of solid state NMR chemical shifts and lineshapes, in 1D or multidimensional spectra, can also provide valuable qualitative information about secondary structure, site-specific order and disorder, and relative populations of distinct structural components. By examining proteins in frozen solutions, averaging of spectroscopic parameters by conformational exchange processes is avoided, allowing clear separations of structural components to be made.

One major impediment to structural studies of partially folded and unfolded proteins has been the low sensitivity of solid state NMR measurements, exacerbated by the relatively broad NMR lines that are intrinsic to disordered systems. Experiments on HP35 have been aided by the fact that protein concentrations of 5 mM or more can be achieved without aggregation, even in thermally unfolded and chemically denatured states. At lower concentrations, the same measurements would become prohibitively time-consuming. However, this situation will likely improve dramatically in the near future, as ultra-low-temperature MAS technology is developed [127] and combined with dynamic nuclear polarization techniques [128]. Sensitivity enhancements by factors of 100–1000 are expected, making solid state NMR measurements on frozen solutions with sub-millimolar protein concentrations not only feasible but also rapid.

In principle, there is no molecular weight limit on protein folding studies by solid state NMR, provided that sufficient protein concentrations can be achieved. In practice, due to the inhomogeneously broadened NMR lines of partially folded and unfolded proteins, isotopic labeling of specific sites is required. This is most easily done when the protein can be synthesized. Alternatively, proteins can be expressed in bacteria with selectively labeled culture media. Even when each amino acid occurs several times within the protein sequence, signals from specific sites can be selected if certain sequential pairs of amino acids occur uniquely. When combined with the advances in sensitivity mentioned above, modern synthesis, ligation, and expression techniques may allow folding processes of proteins in the 10–20 kDa range to be studied by solid state NMR.

In the case of non-equilibrium experiments, folding events or other conformational changes could be triggered by sudden changes in parameters other than temperature, including pressure drops, pH jumps, and changes in ionic strength. By combining rapid pressure jump or rapid mixing techniques with rapid freezing, it should be possible to characterize the ensuing structural evolution by solid state NMR. Processes in which natively unfolded polypeptides adopt well-defined conformations through interactions with protein partners could also be studied in this way. For the full time course of a folding process (e.g., conversion of the partially folded state of HP35 discussed above to the fully folded state) to be accessible, techniques for inserting variable time delays between the initiation step and the freezing step need to be developed. Thus, future progress in the application of solid state NMR to protein folding problems will most likely involve technological developments in several areas. Results obtained to date indicate that such technological efforts will produce a wealth of new information.

Acknowledgement

This work has been supported by the Intramural Research Program of the National Institute of Diabetes and Digestive and Kidney Diseases, a component of the National Institutes of Health.

References

[1] J. Kubelka, T.K. Chiu, D.R. Davies, W.A. Eaton, J. Hofrichter, Sub-microsecond protein folding, J. Mol. Biol. 359 (2006) 546–553.
[2] J. Kubelka, W.A. Eaton, J. Hofrichter, Experimental tests of villin subdomain folding simulations, J. Mol. Biol. 329 (2003) 625–630.
[3] R. Narayanan, L. Pelakh, S.J. Hagen, Solvent friction changes the folding pathway of the tryptophan zipper TZ2, J. Mol. Biol. 390 (2009) 538–546.
[4] L. Pollack, M.W. Tate, N.C. Darnton, J.B. Knight, S.M. Gruner, W.A. Eaton, R.H. Austin, Compactness of the denatured state of a fast-folding protein measured by submillisecond small-angle X-ray scattering, Proc. Natl. Acad. Sci. U. S. A. 96 (1999) 10115–10117.
[5] D.J. Segel, A. Bachmann, J. Hofrichter, K.O. Hodgson, S. Doniach, T. Kiefhaber, Characterization of transient intermediates in lysozyme folding with time-resolved small-angle X-ray scattering, J. Mol. Biol. 288 (1999) 489–499.
[6] J. Woenckhaus, R. Kohling, P. Thiyagarajan, K.C. Littrell, S. Seifert, C.A. Royer, R. Winter, Pressure-jump small-angle X-ray scattering detected kinetics of staphylococcal nuclease folding, Biophys. J. 80 (2001) 1518–1523.
[7] W.Y. Yang, M. Gruebele, Folding at the speed limit, Nature 423 (2003) 193–197.
[8] V.L. Arcus, S. Vuilleumier, S.M.V. Freund, M. Bycroft, A.R. Fersht, A comparison of the pH, urea, and temperature-denatured states of barnase by heteronuclear NMR: implications for the initiation of protein folding, J. Mol. Biol. 254 (1995) 305–321.
[9] S. Cavagnero, C. Nishimura, S. Schwarzinger, H.J. Dyson, P.E. Wright, Conformational and dynamic characterization of the molten globule state of an apomyoglobin mutant with an altered folding pathway, Biochemistry 40 (2001) 14459–14467.
[10] W. Fieber, S. Kristjansdottir, F.M. Poulsen, Short-range, long-range and transition state interactions in the denatured state of ACBP from residual dipolar couplings, J. Mol. Biol. 339 (2004) 1191–1199.
[11] K.M. Fiebig, H. Schwalbe, M. Buck, L.J. Smith, C.M. Dobson, Toward a description of the conformations of denatured states of proteins. Comparison of a random coil model with NMR measurements, J. Phys. Chem. 100 (1996) 2661–2666.
[12] J.R. Gillespie, D. Shortle, Characterization of long-range structure in the denatured state of staphylococcal nuclease. 2. Distance restraints from paramagnetic

relaxation and calculation of an ensemble of structures, J. Mol. Biol. 268 (1997) 170–184.
[13] M.R. Jensen, P.R.L. Markwick, S. Meier, C. Griesinger, M. Zweckstetter, S. Grzesiek, P. Bernado, M. Blackledge, Quantitative determination of the conformational properties of partially folded and intrinsically disordered proteins using NMR dipolar couplings, Structure 17 (2009) 1169–1185.
[14] T. Kortemme, M.J.S. Kelly, L.E. Kay, J. Forman-Kay, L. Serrano, Similarities between the spectrin sH3 domain denatured state and its folding transition state, J. Mol. Biol. 297 (2000) 1217–1229.
[15] S. Kristjansdottir, K. Lindorff-Larsen, W. Fieber, C.M. Dobson, M. Vendruscolo, F.M. Poulsen, Formation of native and non-native interactions in ensembles of denatured ACBP molecules from paramagnetic relaxation enhancement studies, J. Mol. Biol. 347 (2005) 1053–1062.
[16] J.A. Marsh, C. Neale, F.E. Jack, W.Y. Choy, A.Y. Lee, K.A. Crowhurst, J.D. Forman-Kay, Improved structural characterizations of the DRKN sH3 domain unfolded state suggest a compact ensemble with native-like and non-native structure, J. Mol. Biol. 367 (2007) 1494–1510.
[17] J.A. Marsh, V.K. Singh, Z.C. Jia, J.D. Forman-Kay, Sensitivity of secondary structure propensities to sequence differences between alpha- and gamma-synuclein: Implications for fibrillation, Protein Sci. 15 (2006) 2795–2804.
[18] U. Mayor, J.G. Grossmann, N.W. Foster, S.M.V. Freund, A.R. Fersht, The denatured state of engrailed homeodomain under denaturing and native conditions, J. Mol. Biol. 333 (2003) 977–991.
[19] S. Meier, S. Grzesiek, M. Blackledge, Mapping the conformational landscape of urea-denatured ubiquitin using residual dipolar couplings, J. Am. Chem. Soc. 129 (2007) 9799–9807.
[20] M.D. Mukrasch, P. Markwick, J. Biernat, M. von Bergen, P. Bernado, C. Griesinger, E. Mandelkow, M. Zweckstetter, M. Blackledge, Highly populated turn conformations in natively unfolded tau protein identified from residual dipolar couplings and molecular simulation, J. Am. Chem. Soc. 129 (2007) 5235–5243.
[21] S. Ohnishi, A.L. Lee, M.H. Edgell, D. Shortle, Direct demonstration of structural similarity between native and denatured eglin C, Biochemistry 43 (2004) 4064–4070.
[22] H. Schwalbe, K.M. Fiebig, M. Buck, J.A. Jones, S.B. Grimshaw, A. Spencer, S.J. Glaser, L.J. Smith, C.M. Dobson, Structural and dynamical properties of a denatured protein. Heteronuclear 3D NMR experiments and theoretical simulations of lysozyme in 8 M urea, Biochemistry 36 (1997) 8977–8991.
[23] S. Schwarzinger, P.E. Wright, H.J. Dyson, Molecular hinges in protein folding: the urea-denatured state of apomyoglobin, Biochemistry 41 (2002) 12681–12686.
[24] L.J. Smith, K.A. Bolin, H. Schwalbe, M.W. MacArthur, J.M. Thornton, C.M. Dobson, Analysis of main chain torsion angles in proteins: prediction of NMR coupling constants for native and random coil conformations, J. Mol. Biol. 255 (1996) 494–506.
[25] K.N. Hu, W.M. Yau, R. Tycko, Detection of a transient intermediate in a rapid protein folding process by solid state nuclear magnetic resonance, J. Am. Chem. Soc. 132 (2010) 24–25.
[26] K.N. Hu, R.H. Havlin, W.M. Yau, R. Tycko, Quantitative determination of site-specific conformational distributions in an unfolded protein by solid state nuclear magnetic resonance, J. Mol. Biol. 392 (2009) 1055–1073.
[27] R.H. Havlin, R. Tycko, Probing site-specific conformational distributions in protein folding with solid state NMR, Proc. Natl. Acad. Sci. U. S. A. 102 (2005) 3284–3289.
[28] H.W. Long, R. Tycko, Biopolymer conformational distributions from solid state NMR: α-helix and 3_{10}-helix contents of a helical peptide, J. Am. Chem. Soc. 120 (1998) 7039–7048.
[29] J. Schaefer, E.O. Stejskal, ^{13}C nuclear magnetic-resonance of polymers spinning at magic angle, J. Am. Chem. Soc. 98 (1976) 1031–1032.
[30] I.J. Lowe, Free induction decays of rotating solids, Phys. Rev. Lett. 2 (1959) 285–287.
[31] E.R. Andrew, A. Bradbury, R.G. Eades, Nuclear magnetic resonance spectra from a crystal rotated at high speed, Nature 182 (1958) 1659.
[32] E.O. Stejskal, J. Schaefer, J.S. Waugh, Magic-angle spinning and polarization transfer in proton-enhanced NMR, J. Magn. Reson. 28 (1977) 105–112.
[33] A. Pines, M.G. Gibby, J.S. Waugh, Proton-enhanced NMR of dilute spins in solids, J. Chem. Phys. 59 (1973) 569–590.
[34] S.R. Hartmann, E.L. Hahn, Nuclear double resonance in rotating frame, Phys. Rev. 128 (1962) 2042–2053.
[35] C.P. Jaroniec, B.A. Tounge, J. Herzfeld, R.G. Griffin, Frequency selective heteronuclear dipolar recoupling in rotating solids: accurate 13C–15 N distance measurements in uniformly 13C, 15 N-labeled peptides, J. Am. Chem. Soc. 123 (2001) 3507–3519.
[36] A.E. Bennett, C.M. Rienstra, J.M. Griffiths, W.G. Zhen, P.T. Lansbury, R.G. Griffin, Homonuclear radio frequency-driven recoupling in rotating solids, J. Chem. Phys. 108 (1998) 9463–9479.
[37] M. Hohwy, H.J. Jakobsen, M. Eden, M.H. Levitt, N.C. Nielsen, Broadband dipolar recoupling in the nuclear magnetic resonance of rotating solids: a compensated C7 pulse sequence, J. Chem. Phys. 108 (1998) 2686–2694.
[38] D.M. Gregory, D.J. Mitchell, J.A. Stringer, S. Kiihne, J.C. Shiels, J. Callahan, M.A. Mehta, G.P. Drobny, Windowless dipolar recoupling: the detection of weak dipolar couplings between spin-1/2 nuclei with large chemical shift anisotropies, Chem. Phys. Lett. 246 (1995) 654–663.
[39] R. Tycko, G. Dabbagh, Measurement of nuclear magnetic dipole–dipole couplings in magic-angle spinning NMR, Chem. Phys. Lett. 173 (1990) 461–465.
[40] R. Tycko, G. Dabbagh, P.A. Mirau, Determination of chemical shift anisotropy lineshapes in a two-dimensional magic-angle spinning NMR experiment, J. Magn. Reson. 85 (1989) 265–274.
[41] T. Gullion, J. Schaefer, Rotational-echo double-resonance NMR, J. Magn. Reson. 81 (1989) 196–200.
[42] D.P. Raleigh, M.H. Levitt, R.G. Griffin, Rotational resonance in solid state NMR, Chem. Phys. Lett. 146 (1988) 71–76.
[43] B.H. Meier, W.L. Earl, Excitation of multiple quantum transitions under magic angle spinning conditions: adamantane, J. Chem. Phys. 85 (1986) 4905–4911.
[44] M.A. Alla, E.I. Kundla, E.T. Lippmaa, Selective determination of anisotropic magnetic interactions from high-resolution NMR spectra of powdered samples, JETP Lett. 27 (1978) 194–197.
[45] R. Tycko, Symmetry-based constant-time homonuclear dipolar recoupling in solid state NMR, J. Chem. Phys. 126 (2007).
[46] K. Schmidt-Rohr, W. Hu, N. Zumbulyadis, Elucidation of the chain conformation in a glassy polyester, PET, by two-dimensional NMR, Science 280 (1998) 714–717.
[47] M. Hong, J.D. Gross, R.G. Griffin, Site-resolved determination of peptide torsion angle ϕ from the relative orientations of backbone N–H and C–H bonds by solid state NMR, J. Phys. Chem. B 101 (1997) 5869–5874.
[48] X. Feng, Y.K. Lee, D. Sandstrom, M. Eden, H. Maisel, A. Sebald, M.H. Levitt, Direct determination of a molecular torsional angle by solid state NMR, Chem. Phys. Lett. 257 (1996) 314–320.
[49] F.J. Blanco, R. Tycko, Determination of polypeptide backbone dihedral angles in solid state NMR by double quantum ^{13}C chemical shift anisotropy measurements, J. Magn. Reson. 149 (2001) 131–138.
[50] R. Tycko, A.E. Berger, Dual processing of two-dimensional exchange data in magic-angle spinning NMR of solids, J. Magn. Reson. 141 (1999) 141–147.
[51] P.M. Henrichs, M. Linder, ^{13}C spin diffusion in the determination of intermolecular structure in solids, J. Magn. Reson. 58 (1984) 458–461.
[52] R. Tycko, D.P. Weliky, A.E. Berger, Investigation of molecular structure in solids by two-dimensional NMR exchange spectroscopy with magic-angle spinning, J. Chem. Phys. 105 (1996) 7915–7930.
[53] D.P. Weliky, R. Tycko, Determination of peptide conformations by two-dimensional magic-angle spinning NMR exchange spectroscopy with rotor synchronization, J. Am. Chem. Soc. 118 (1996) 8487–8488.
[54] J.C.C. Chan, R. Tycko, Solid state NMR spectroscopy method for determination of the backbone torsion angle ψ in peptides with isolated uniformly labeled residues, J. Am. Chem. Soc. 125 (2003) 11828–11829.
[55] Y. Ishii, T. Terao, M. Kainosho, Relayed anisotropy correlation NMR: determination of dihedral angles in solids, Chem. Phys. Lett. 256 (1996) 133–140.
[56] D.P. Weliky, G. Dabbagh, R. Tycko, Correlation of chemical bond directions and functional group orientations in solids by two-dimensional NMR, J. Magn. Reson. Ser. A 104 (1993) 10–16.
[57] S. Luca, D.V. Filippov, J.H. van Boom, H. Oschkinat, H.J.M. de Groot, M. Baldus, Secondary chemical shifts in immobilized peptides and proteins: A qualitative basis for structure refinement under magic-angle spinning, J. Biomol. NMR 20 (2001) 325–331.
[58] Y. Ishii, ^{13}C–^{13}C dipolar recoupling under very fast magic-angle spinning in solid state nuclear magnetic resonance: applications to distance measurements, spectral assignments, and high-throughput secondary structure determination, J. Chem. Phys. 114 (2001) 8473–8483.
[59] J.J. Balbach, Y. Ishii, O.N. Antzutkin, R.D. Leapman, N.W. Rizzo, F. Dyda, J. Reed, R. Tycko, Amyloid fibril formation by $A\beta_{16-22}$, a seven-residue fragment of the Alzheimer's β-amyloid peptide, and structural characterization by solid state NMR, Biochemistry 39 (2000) 13748–13759.
[60] C.R. Morcombe, V. Gaponenko, R.A. Byrd, K.W. Zilm, Diluting abundant spins by isotope edited radio frequency field assisted diffusion, J. Am. Chem. Soc. 126 (2004) 7196–7197.
[61] R. Tycko, Y. Ishii, Constraints on supramolecular structure in amyloid fibrils from two-dimensional solid state NMR spectroscopy with uniform isotopic labeling, J. Am. Chem. Soc. 125 (2003) 6606–6607.
[62] A. Lange, S. Luca, M. Baldus, Structural constraints from proton-mediated rare-spin correlation spectroscopy in rotating solids, J. Am. Chem. Soc. 124 (2002) 9704–9705.
[63] K. Takegoshi, S. Nakamura, T. Terao, ^{13}C–^{1}H dipolar-assisted rotational resonance in magic-angle spinning NMR, Chem. Phys. Lett. 344 (2001) 631–637.
[64] I. Bertini, A. Bhaumik, G. De Paepe, R.G. Griffin, M. Lelli, J.R. Lewandowski, C. Luchinat, High-resolution solid state NMR structure of a 17.6 kDa protein, J. Am. Chem. Soc. 132 (2010) 1032–1040.
[65] P.S. Nadaud, J.J. Helmus, S.L. Kall, C.P. Jaroniec, Paramagnetic ions enable tuning of nuclear relaxation rates and provide long range structural restraints in solid state NMR of proteins, J. Am. Chem. Soc. 131 (2009) 8108–8120.
[66] A.J. Nieuwkoop, B.J. Wylie, W.T. Franks, G.J. Shah, C.M. Rienstra, Atomic resolution protein structure determination by three-dimensional transferred echo double resonance solid state nuclear magnetic resonance spectroscopy, J. Chem. Phys. 131 (2009).
[67] A. Loquet, B. Bardiaux, C. Gardiennet, C. Blanchet, M. Baldus, M. Nilges, T. Malliavin, A. Bockmann, 3D structure determination of the Crh protein from highly ambiguous solid state NMR restraints, J. Am. Chem. Soc. 130 (2008) 3579–3589.
[68] S.G. Zech, A.J. Wand, A.E. McDermott, Protein structure determination by high-resolution solid state NMR spectroscopy: application to microcrystalline ubiquitin, J. Am. Chem. Soc. 127 (2005) 8618–8626.
[69] F. Castellani, B. van Rossum, A. Diehl, M. Schubert, K. Rehbein, H. Oschkinat, Structure of a protein determined by solid state magic-angle-spinning NMR spectroscopy, Nature 420 (2002) 98–102.
[70] A.K. Paravastu, R.D. Leapman, W.M. Yau, R. Tycko, Molecular structural basis for polymorphism in Alzheimer's β-amyloid fibrils, Proc. Natl. Acad. Sci. U. S. A. 105 (2008) 18349–18354.
[71] C. Wasmer, A. Lange, H. Van Melckebeke, A.B. Siemer, R. Riek, B.H. Meier, Amyloid fibrils of the HET-s(218–289) prion form a β-solenoid with a triangular hydrophobic core, Science 319 (2008) 1523–1526.

[72] S. Luca, W.M. Yau, R. Leapman, R. Tycko, Peptide conformation and supramolecular organization in amylin fibrils: constraints from solid state NMR, Biochemistry 46 (2007) 13505–13522.
[73] F. Shewmaker, R.B. Wickner, R. Tycko, Amyloid of the prion domain of Sup35p has an in-register parallel β-sheet structure, Proc. Natl. Acad. Sci. U. S. A. 103 (2006) 19754–19759.
[74] R. Tycko, Molecular structure of amyloid fibrils: insights from solid state NMR, Q. Rev. Biophys. 39 (2006) 1–55.
[75] A.T. Petkova, W.M. Yau, R. Tycko, Experimental constraints on quaternary structure in Alzheimer's β-amyloid fibrils, Biochemistry 45 (2006) 498–512.
[76] C.P. Jaroniec, C.E. MacPhee, V.S. Bajaj, M.T. McMahon, C.M. Dobson, R.G. Griffin, High-resolution molecular structure of a peptide in an amyloid fibril determined by magic-angle spinning NMR spectroscopy, Proc. Natl. Acad. Sci. U. S. A. 101 (2004) 711–716.
[77] A.T. Petkova, G. Buntkowsky, F. Dyda, R.D. Leapman, W.M. Yau, R. Tycko, Solid state NMR reveals a pH-dependent antiparallel β-sheet registry in fibrils formed by a β-amyloid peptide, J. Mol. Biol. 335 (2004) 247–260.
[78] S.H. Park, A.A. Mrse, A.A. Nevzorov, M.F. Mesleh, M. Oblatt-Montal, M. Montal, S.J. Opella, Three-dimensional structure of the channel-forming trans-membrane domain of virus protein "U" (Vpu) from HIV-1, J. Mol. Biol. 333 (2003) 409–424.
[79] J.F. Wang, S. Kim, F. Kovacs, T.A. Cross, Structure of the transmembrane region of the M2 protein H + channel, Protein Sci. 10 (2001) 2241–2250.
[80] S.J. Opella, F.M. Marassi, J.J. Gesell, A.P. Valente, Y. Kim, M. Oblatt-Montal, M. Montal, Structures of the M2 channel-lining segments from nicotinic acetylcholine and NMDA receptors by NMR spectroscopy, Nat. Struct. Biol. 6 (1999) 374–379.
[81] R.R. Ketchem, W. Hu, T.A. Cross, High-resolution conformation of gramicidin A in a lipid bilayer by solid state NMR, Science 261 (1993) 1457–1460.
[82] D.H. Juers, B.W. Matthews, Cryo-cooling in macromolecular crystallography: advantages, disadvantages and optimization, Q. Rev. Biophys. 37 (2004) 105–119.
[83] B. Halle, Biomolecular cryocrystallography: structural changes during flash-cooling, Proc. Natl. Acad. Sci. U. S. A. 101 (2004) 4793–4798.
[84] R.F. Tilton, J.C. Dewan, G.A. Petsko, Effects of temperature on protein structure and dynamics: X-ray crystallographic studies of the protein ribonuclease A at nine different temperatures from 98 K to 320 K, Biochemistry 31 (1992) 2469–2481.
[85] S. Marqusee, V.H. Robbins, R.L. Baldwin, Unusually stable helix formation in short alanine-based peptides, Proc. Natl. Acad. Sci. U. S. A. 86 (1989) 5286–5290.
[86] G.L. Millhauser, Views of helical peptides: a proposal for the position of 3_{10} helix along the thermodynamic folding pathway, Biochemistry 34 (1995) 3873–3877.
[87] C.J. McKnight, D.S. Doering, P.T. Matsudaira, P.S. Kim, A thermostable 35-residue subdomain within villin headpiece, J. Mol. Biol. 260 (1996) 126–134.
[88] C.J. McKnight, P.T. Matsudaira, P.S. Kim, NMR structure of the 35-residue villin headpiece subdomain, Nat. Struct. Biol. 4 (1997) 180–184.
[89] J.M. Meng, D. Vardar, Y.M. Wang, H.C. Guo, J.F. Head, C.J. McKnight, High-resolution crystal structures of villin headpiece and mutants with reduced F-actin binding activity, Biochemistry 44 (2005) 11963–11973.
[90] T.K. Chiu, J. Kubelka, R. Herbst-Irmer, W.A. Eaton, J. Hofrichter, D.R. Davies, High-resolution X-ray crystal structures of the villin headpiece subdomain, an ultrafast folding protein, Proc. Natl. Acad. Sci. U. S. A. 102 (2005) 7517–7522.
[91] V. Munoz, L. Serrano, Development of the multiple sequence approximation within the AGADIR model of α-helix formation: comparison with Zimm–Bragg and Lifson–Roig formalisms, Biopolymers 41 (1997) 495–509.
[92] B.S. Frank, D. Vardar, D.A. Buckley, C.J. McKnight, The role of aromatic residues in the hydrophobic core of the villin headpiece subdomain, Protein Sci. 11 (2002) 680–687.
[93] J. Kubelka, E.R. Henry, T. Cellmer, J. Hofrichter, W.A. Eaton, Chemical, physical, and theoretical kinetics of an ultrafast folding protein, Proc. Natl. Acad. Sci. U. S. A. 105 (2008) 18655–18662.
[94] T. Cellmer, E.R. Henry, J. Kubelka, J. Hofrichter, W.A. Eaton, Relaxation rate for an ultrafast folding protein is independent of chemical denaturant concentration, J. Am. Chem. Soc. 129 (2007) 14564–14565.
[95] M.H. Wang, Y.F. Tang, S.S. Sato, L. Vugmeyster, C.J. McKnight, D.P. Raleigh, Dynamic NMR lineshape analysis demonstrates that the villin headpiece subdomain folds on the microsecond time scale, J. Am. Chem. Soc. 125 (2003) 6032–6033.
[96] S.H. Brewer, B.B. Song, D.P. Raleigh, R.B. Dyer, Residue specific resolution of protein folding dynamics using isotope-edited infrared temperature jump spectroscopy, Biochemistry 46 (2007) 3279–3285.
[97] J.S. Yang, S. Wallin, E.I. Shakhnovich, Universality and diversity of folding mechanics for three-helix bundle proteins, Proc. Natl. Acad. Sci. U. S. A. 105 (2008) 895–900.
[98] B. Zagrovic, V.S. Pande, Simulated unfolded-state ensemble and the experimental NMR structures of villin headpiece yield similar wide-angle solution X-ray scattering profiles, J. Am. Chem. Soc. 128 (2006) 11742–11743.
[99] S.M. Jang, E. Kim, S. Shin, Y. Pak, Ab initio folding of helix bundle proteins using molecular dynamics simulations, J. Am. Chem. Soc. 125 (2003) 14841–14846.
[100] A. Fernandez, M.Y. Shen, A. Colubri, T.R. Sosnick, R.S. Berry, K.F. Freed, Large scale context in protein folding: villin headpiece, Biochemistry 42 (2003) 664–671.
[101] M.Y. Shen, K.F. Freed, All-atom fast protein folding simulations: the villin headpiece, Proteins 49 (2002) 439–445.
[102] B. Zagrovic, C.D. Snow, M.R. Shirts, V.S. Pande, Simulation of folding of a small α-helical protein in atomistic detail using worldwide distributed computing, J. Mol. Biol. 323 (2002) 927–937.
[103] S.A. Islam, M. Karplus, D.L. Weaver, Application of the diffusion–collision model to the folding of three-helix bundle proteins, J. Mol. Biol. 318 (2002) 199–215.
[104] D.C. Sullivan, I.D. Kuntz, Protein folding as biased conformational diffusion, J. Phys. Chem. B 106 (2002) 3255–3262.
[105] Y. Duan, L. Wang, P.A. Kollman, The early stage of folding of villin headpiece subdomain observed in a 200-nanosecond fully solvated molecular dynamics simulation, Proc. Natl. Acad. Sci. U. S. A. 95 (1998) 9897–9902.
[106] P.L. Freddolino, K. Schulten, Common structural transitions in explicit-solvent simulations of villin headpiece folding, Biophys. J. 97 (2009) 2338–2347.
[107] A.E. Bennett, D.P. Weliky, R. Tycko, Quantitative conformational measurements in solid state NMR by constant-time homonuclear dipolar recoupling, J. Am. Chem. Soc. 120 (1998) 4897–4898.
[108] S.J. Whittington, B.W. Chellgren, V.M. Hermann, T.P. Creamer, Urea promotes polyproline II helix formation: implications for protein denatured states, Biochemistry 44 (2005) 6269–6275.
[109] Z.S. Shi, K. Chen, Z.G. Liu, A. Ng, W.C. Bracken, N.R. Kallenbach, Polyproline II propensities from GGXGG peptides reveal an anticorrelation with β-sheet scales, Proc. Natl. Acad. Sci. U. S. A. 102 (2005) 17964–17968.
[110] S.A. Asher, A.V. Mikhonin, S. Bykov, UV raman demonstrates that α-helical polyalanine peptides melt to polyproline II conformations, J. Am. Chem. Soc. 126 (2004) 8433–8440.
[111] J.C. Ferreon, V.J. Hilser, The effect of the polyproline II (PPII) conformation on the denatured state entropy, Protein Sci. 12 (2003) 447–457.
[112] Z.S. Shi, C.A. Olson, G.D. Rose, R.L. Baldwin, N.R. Kallenbach, Polyproline II structure in a sequence of seven alanine residues, Proc. Natl. Acad. Sci. U. S. A. 99 (2002) 9190–9195.
[113] R.K. Dukor, T.A. Keiderling, Reassessment of the random coil conformation: vibrational CD study of proline oligopeptides and related polypeptides, Biopolymers 31 (1991) 1747–1761.
[114] M. Mezei, P.J. Fleming, R. Srinivasan, G.D. Rose, Polyproline II helix is the preferred conformation for unfolded polyalanine in water, Proteins Struct. Funct. Bioinform. 55 (2004) 502–507.
[115] A. Kentsis, M. Mezei, T. Gindin, R. Osman, Unfolded state of polyalanine is a segmented polyproline II helix, Proteins Struct. Funct. Bioinform. 55 (2004) 493–501.
[116] Y. Lin, G.J. Gerfen, D.L. Rousseau, S.R. Yeh, Ultrafast microfluidic mixer and freeze-quenching device, Anal. Chem. 75 (2003) 5381–5386.
[117] A. Cherepanov, S. de Vries, Microsecond freeze-hyperquenching: development of a new ultrafast micro-mixing and sampling technology and application to enzyme catalysis, Biochim. Biophys. Acta 1656 (2004) 1–31.
[118] R.J. Appleyard, W.A. Shuttleworth, J.N.S. Evans, Time-resolved solid state NMR spectroscopy of 5-enolpyruvylshikimate-3-phosphate synthase, Biochemistry 33 (1994) 6812–6821.
[119] M. Etzkorn, A. Bockmann, F. Penin, D. Riedel, M. Baldus, Characterization of folding intermediates of a domain-swapped protein by solid state NMR spectroscopy, J. Am. Chem. Soc. 129 (2007) 169–175.
[120] S. Chimon, M.A. Shaibat, C.R. Jones, D.C. Calero, B. Aizezi, Y. Ishii, Evidence of fibril-like β-sheet structures in a neurotoxic amyloid intermediate of Alzheimer's β-amyloid, Nat. Struct. Mol. Biol. 14 (2007) 1157–1164.
[121] J.W. Wu, L. Breydo, J.M. Isas, J. Lee, Y.G. Kuznetsov, R. Langen, C. Glabe, Fibrillar oligomers nucleate the oligomerization of monomeric amyloid β but do not seed fibril formation, J. Biol. Chem. 285 (2010) 6071–6079.
[122] M.L. Mak-Jurkauskas, V.S. Bajaj, M.K. Hornstein, M. Belenky, R.G. Griffin, J. Herzfeld, Energy transformations early in the bacteriorhodopsin photocycle revealed by DNP-enhanced solid state NMR, Proc. Natl. Acad. Sci. U. S. A. 105 (2008) 883–888.
[123] J.C. Lansing, M. Hohwy, C.P. Jaroniec, A.F.L. Creemers, J. Lugtenburg, J. Herzfeld, R.G. Griffin, Chromophore distortions in the bacteriorhodopsin photocycle: evolution of the H–C14–C15–H dihedral angle measured by solid state NMR, Biochemistry 41 (2002) 431–438.
[124] V. Hornak, S. Ahuja, M. Eilers, J.A. Goncalves, M. Sheves, P.J. Reeves, S.O. Smith, Light activation of rhodopsin: Insights from molecular dynamics simulations guided by solid state NMR distance restraints, J. Mol. Biol. 396 (2010) 510–527.
[125] X. Feng, P.J.E. Verdegem, M. Eden, D. Sandstrom, Y.K. Lee, P.H.M. Bovee-Geurts, W.J. de Grip, J. Lugtenburg, H.J.M. de Groot, M.H. Levitt, Determination of a molecular torsional angle in the metarhodopsin-I photointermediate of rhodopsin by double-quantum solid state NMR, J. Biomol. NMR 16 (2000) 1–8.
[126] M. Utz, Measurement of structural distribution functions in disordered systems: a general approach for sensitivity estimation, J. Chem. Phys. 109 (1998) 6110–6124.
[127] K.R. Thurber, R. Tycko, Biomolecular solid state NMR with magic-angle spinning at 25 K, J. Magn. Reson. 195 (2008) 179–186.
[128] T. Maly, G.T. Debelouchina, V.S. Bajaj, K.N. Hu, C.G. Joo, M.L. Mak-Jurkauskas, J.R. Sirigiri, P.C.A. van der Wel, J. Herzfeld, R.J. Temkin, R.G. Griffin, Dynamic nuclear polarization at high magnetic fields, J. Chem. Phys. 128 (2008).